Journal of Molecular Structure 1132 (2017) 175–180

Contents lists available at ScienceDirect

Journal of Molecular Structure

journal homepage: http://www.elsevier.com/locate/molstruc

Gas and crystal structures of CCl_2FSCN☆

Yanina Berrueta Martínez [a], Lucas S. Rodríguez Pirani [a], Mauricio F. Erben [a], Roland Boese [c], Christian G. Reuter [b], Yury V. Vishnevskiy [b], Norbert W. Mitzel [b, **], Carlos O. Della Védova [a, *]

[a] CEQUINOR (UNLP-CONICET), Departamento de Química, Facultad de Ciencias Exactas, Universidad Nacional de La Plata, 47 esq. 115, 1900 La Plata, Argentina
[b] Lehrstuhl für Anorganische Chemie und Strukturchemie, Universität Bielefeld, Universitätsstraße 25, 33615 Bielefeld, Germany
[c] Strukturchemie-Institut für Anorganische Chemie, Universität Duisburg Essen, Universitätsstraße 7, 45117 Essen, Germany

ARTICLE INFO

Article history:
Received 25 January 2016
Received in revised form
25 March 2016
Accepted 28 March 2016
Available online 30 March 2016

Keywords:
Dichlorofluoromethyl thiocyanate
Gas electron diffraction
X-ray diffraction

ABSTRACT

Dichlorofluoromethyl thiocyanate, CCl_2FSCN, was structurally studied in the solid and in the gas phase by means of single-crystal X-ray (XRD) and gas electron diffraction (GED), respectively. In the gas phase the title molecule adopts two stable conformers, described by the FC–SC dihedral angle. The *gauche*-conformer (FC bond with respect to the SC bond) is more stable than the *anti*-conformer. In this work we present the first experimental evidence for the existence of the *anti*-CF_2ClSCN form. In the solid state only the most stable *gauche*-conformer was found. Intermolecular interactions were detected in the crystal structure and analyzed. A structural comparison of the results with those of related species as CCl_2FSCN, CCl_3SCN and CH_2ClSCN is presented.

1. Introduction

The family of thiocyanate compounds is under permanent investigation. Some experimental IR and Raman spectroscopy data as well as theoretical investigations for this species have been reported twenty years ago by our group [1]. In this work, *gauche*-CCl_2FSCN was experimentally detected by means of Raman polarization measurements supplemented by computational chemistry calculations. On the other hand, the *anti*-conformer could only be computed by quantum-chemical calculations. Experimental support for the less stable *anti*-conformer is now finally provided by the gas phase electron diffraction study presented in this work. Complementarily, X-ray diffraction measurements allow determining the crystal structure of the less symmetric and more abundant *gauche*-conformer. Some intermolecular interactions in terms of geometrical parameters involving halogen and chalcogen atoms have been determined. Finally, a comparison of the gas and crystal-phase structures between CCl_2FSCN, CCl_3SCN [2] and CH_2ClSCN [3] is presented.

2. Experimental section

2.1. Synthesis

CCl_2FSCN was prepared by the reaction of CCl_2FSCl with KCN in ether [4]. Purification was performed by several trap-to-trap distillations [5]. The identity and purity of dichlorofluoromethyl thiocyanate were verified using infrared spectroscopy.

2.2. Instrumentation and procedure

2.2.1. Quantum-chemical calculations

The Gaussian 03 suite of programs [6] was used to compute DFT [7] and MP2 [8] calculations. The existence of minima on the potential hyper-surface was proved computing the corresponding harmonic frequencies after each geometry optimization. For the GED structural analyses analytical harmonic and numeric cubic force fields were calculated at the B3LYP/6-31G(d) and O3LYP/cc-pVTZ levels of the theory. These results were then used to calculate mean-square interatomic vibrational amplitudes and vibrational corrections to the equilibrium structure by the SHRINK program [9–11]. Coupled-cluster CCSD and CCSD(T) [12] analytical

☆ Dedicated to Prof. Dr. Georgiy Vasil'evich Girichev on occasion of his 70th anniversary on January 13, 2017.

* Corresponding author.
** Corresponding author.
E-mail address: carlosdv@quimica.unlp.edu.ar (C.O. Della Védova).

http://dx.doi.org/10.1016/j.molstruc.2016.03.097
0022-2860/

gradient-powered geometry optimizations were performed using the Cfour program package [13].

In order to search the nature of the halogen or chalcogen intermolecular interactions, NBO computational calculations were performed by means of the NBO package contained in the Gaussian 03 program [14]. The second-order perturbation stabilization energies (E) associated to the charge transfer between electron donor and acceptor orbitals corresponding to adjacent molecules were calculated at the NBO B3LYP/6-311 + G(d) level of approximation.

2.2.2. Gas electron diffraction

Gas electron diffraction patterns were measured using the improved Balzers Eldigraph KD-G2 gas-phase electron diffractometer [15] at Bielefeld University. The experimental details are depicted in Table S1. Diffraction images were measured on the Fuji BAS-IP MP2 2025 imaging plates, which subsequently were scanned using the calibrated Fuji BAS-1800II scanner. The intensity curves (see Fig. S1 – S2) were retrieved from the scanned diffraction images by applying the method described earlier [16]. Sector functions and electron wavelengths were calibrated as usually using benzene diffraction patterns, recorded along with the substance under investigation [17]. Experimental amplitudes were refined in groups (see Tables S1 – S2). For this purpose scale factors (one per group) were used as independent parameters. The ratios between different amplitudes in one group were fixed at the theoretical values.

Two sets of theoretical amplitudes and corrections, calculated from B3LYP/6-31G(d) and O3LYP/cc-pVTZ force fields, were tested in the refinements. Those calculated at the B3LYP/6-31G(d) level allowed obtaining better agreement with experimental data and were used in the final models. For CCl_2FSCN, three GED models were used: (a) *anti*-conformation, (b) *gauche*-conformation and (c) a mixture of both conformations. The largest correlations (more than 0.7) obtained were: r(C1–S2)/l1 = 0.82, r(C1–S2)/r(C1–Cl6) = −0.74, <(S2–C1–F5)/χ = −0.73, r(S2–C3)/χ = −0.73. The definitions for groups of refined amplitudes are given in Tables S2 and S3.

2.2.3. X-ray diffraction

Crystallography measurements were carried out at Essen-Duisburg University. A four circle Nicolet R3m/V diffractometer, with a Mo-Kα source (λ = 0.71073 Å) was used [18]. Crystal structures were solved by the Patterson method and refined with SHELXTL-Plus Version SGI IRIS indigo Software [19]. The sample was placed in a 0.2–0.3 mm diameter glass capillary, which was closed at both ends. Using a coupled microscope integrated to the diffractometer, the formation of microcrystals (polycrystalline) was observed while decreasing the temperature of the sample. The sample was cooled at about 15 C below the melting point, and, with a melting zone by zone procedure and subsequent recrystallization caused by heating with an infrared laser focused to a very small area of the sample, a single crystal suitable for an X-ray diffraction experiment grew. A detailed description of this technique is reported in the literature [20]. Table 1 lists the parameters of the XRD experiments.

CCDC 1021027 contains the supplementary crystallographic data for this paper. These data can be obtained free of charge from The Cambridge Crystallographic Data Centre via www.ccdc.cam.ac.uk/data_request/cif.

Table 1
Details of the X-ray diffraction experiments for CCl_2FSCN.

Chemical formula	CCl_2FSCN
M_r	160.0
Unit cell, space group	orthorhombic, $P2_12_12_1$
Temperature (K)	193(1)
a (Å)	5.9327(1)
b (Å)	8.38740(2)
c (Å)	11.5697(1)
β (°)	90
V (Å^3)	575.707(13)
Z	4
ρ_{calc} (calculated) (g cm^{-3})	1.8454
F(000)	312
Crystal color	Colorless
Crystal description	Cylindrical
Wavelength (Å)	0.71073
μ (mm^{-1})	1.38
Crystal size (mm)	0.3
θ range	3.00°–30.47°
Completeness to θ_{max}	84.7%
Index range h, k, l	−8/8, −9/9, −16/16
Transm.$_{max/min}$	0.75/0.70
R before/after correct	0.0746/0.0300
Collected reflections	6628
Independent reflections	1503
R(int)	0.019
Data/restraints/parameters	1461/0/65
Goodness of fit in F^2	1.033
$R1$/w$R2$ [observed refl.]	0.0225/0.0558
Observed refl. with	$I > 2\sigma(I)$
$R1$/w$R2$ (complete data)	0.0234/0.0566
Extinction coefficient	0.005(3)
$\rho_{max/min}$ (e Å^{-3})	0.32/−0.31
CCDC *no.*	1020624

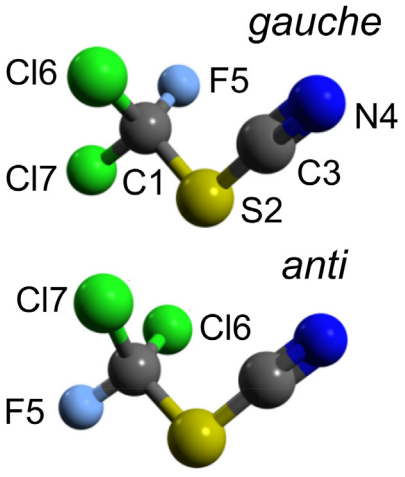

Fig. 1. Molecular structure and atom numbering scheme of the *gauche*- and *anti*-conformers of CCl_2FSCN.

3. Results and discussion

3.1. Computational chemistry

The structure of dichlorofluoromethyl thiocyanate (Fig. 1) was quantum-chemically computed using B3LYP/cc-pVTZ and MP2/cc-pVTZ levels of approximations. The potential-energy functions against the internal rotation around the φ(F–C–S–C) dihedral angle is shown in Fig. 2. As can be seen from Fig. 2, the *gauche*-conformation with a φ(FC–CS) dihedral angle around 60° is more stable than the *anti*-form, with a φ(F–C–C–S) dihedral angle near 180°. Maxima in the potential energy curves are observed for structures with eclipsed orientation between the halogens of CCl_2F and the CN group of thiocyanate SCN.

Despite the qualitative agreement within both methods, the B3LYP level, predicts lower energy barriers than the MP2 method

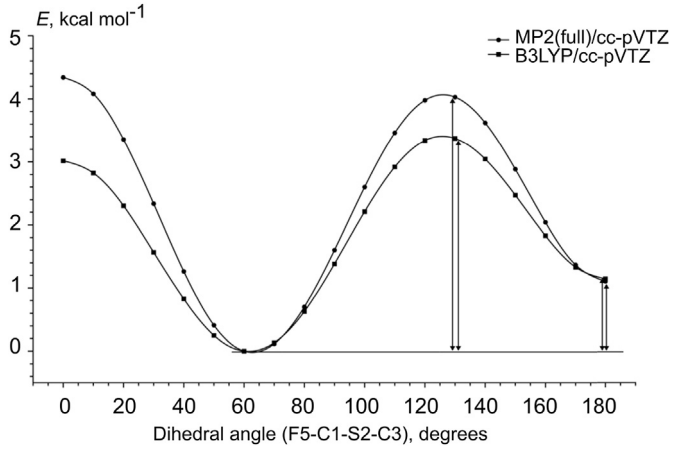

Fig. 2. Potential energy functions of the internal rotation around the φ(F–C–S–C) dihedral angle of CCl_2FSCN.

[21].

The rotational barrier computed for the *gauche*→*anti* conversion in CCl_2FSCN with the mentioned approximation levels agrees with the computed with HF/3-21G*, HF/6-31G* and MP2/6-31G* [1]. Moreover, it is very similar to that obtained in CCl_3SCN [2] and more than twice than the corresponding barrier in CH_2ClSCN [3].

The structures of the two minima were then fully optimized and their frequencies were computed at the same levels of theory. Table 2 lists the relative energies (ΔE) and Gibbs free energies (ΔG^0) along with the conformational population, which was calculated using the Boltzmann distribution taking into account the degeneration of the *gauche*-conformer. The concentration of the *anti*-conformation in CCl_2FSCN (ca. 7%) is about a half than the concentration of an *anti*-rotamer in CH_2ClSCN (between 15 and 18%) [3].

Furthermore, we also applied the most accurate CCSD(T) method to the CCl_2FSCN molecule in order to compute theoretical structures for comparison with the experimental data (see Table 3).

3.2. Molecular structures

The most relevant structural parameters of CCl_2FSCN are given in Table 3.

3.3. Molecular structure in the gas phase

An experimental determination of the gas-phase structure of CCl_2FSCN was determined by means of gas electron diffraction (GED). Relevant geometric parameters obtained by GED, solid state X-ray diffraction (XRD) and computational calculations are listed together in Table 3 for comparison. Different theoretical models (100% *gauche*, 100% *anti* and a mixture of both conformers) were used in the refining process of CCl_2FSCN. The radial distribution function as well as the corresponding structural *R*-factors obtained applying the different models are given in Fig. 3.

Even though the *gauche*-conformer is by far the most abundant, molecules with *anti*-conformation were also detected in the gas phase at the 300 and 315 K (detailed in Table S1). A straightforward estimation of the conformational composition from the radial distribution function is rather difficult in the present case. The N4–F5 contribution of the *anti*-conformer at $r = 4.8$ Å is not as conclusive as in the refining of the equivalent Cl–N contribution in the CH_2ClSCN molecule [3]. The present contribution is difficult to observe not only due to the neighboring broad N4–Cl7 contribution of the *gauche*-conformer but also due to experimental noise (see Fig. 3). On the other hand, all other interatomic distances are similar for the *gauche*- and *anti*-rotamers. Consequently, the value of the least-squares functional in the structural analysis is not sensitive (see Fig. S3) to the changes in conformational composition of CCl_2FSCN. Additional difficulties in the refinement of the conformations ratio arise due to significant correlations as described in the experimental section. The finally refined ratio between *gauche* and *anti*-conformers of CCl_2FSCN in the gas phase at 305 K was 79(11):21(11)%, respectively. The above described experimental results are generally in agreement with the computed values assuming the limited predicting power of the used approximations. Relevant geometric parameters obtained with XRD, GED and theoretical calculations (CCSD(T)/cc-pVTZ) are compared in Table 3.

Table 4 lists a comparison of the geometrical parameters of CH_2ClSCN, CCl_3SCN and CCl_2FSCN. According to our previous work, simple thiocyanates CH_2ClSCN, CCl_3SCN and CCl_2FSCN present similar C≡N bond lengths in the gas phase [2,3]. Moreover, this parameter is rather independent on the conformation. The differences between the C–Cl bond lengths in this series of compounds are not significant. The longest C1–S2 bonds were observed in CCl_3SCN ($r_g = 1.839(2)$ Å) and *anti*-CCl_2FSCN ($r_g = 1.839(13)$ Å); this can be explained by steric repulsions of the CCl_3 or CCl_2F with the SCN group. The *gauche*-conformer of CH_2ClSCN presents the shortest C1–S2 bond. This parameter was found to be dependent on the orientation of the C–Cl bond with respect to the S2–C3 bond; acquiring a higher value for the *anti*-conformation. This is also the case for the CCl_3SCN molecule (see Table 4).

3.4. Molecular structure in the solid state and intermolecular contacts

3.4.1. Crystal structure of CCl_2FSCN

CCl_2FSCN crystallizes in the orthorhombic space group $P2_12_12_1$, and contains four molecules in the unit cell. The molecules in the crystal adopt the *gauche*-conformation with a dihedral angle δ(F–C–S–C) of 61.5(4)° (Fig. 4). The computed dihedral angle (62.0°) also reproduces the crystallographic value.

The most important intermolecular interactions observed in the crystal phase are represented in Fig. 5 and listed in Table 5. Two non-bonding interaction types, N···S (Fig. 5, part b) and N···Cl (part c), determine the arrangement of the title species in the crystal. The N···S contact of 3.19 Å is considerably shorter than the sum of the van der Waals radii of the involved atoms (3.35 Å). The experimental value of the N···S–C angle of 159° together with the results of the NBO calculations computing an interaction between the nitrogen lone pair (as an electron donor) and the σ*(S–C) molecular orbital (as an electron acceptor) allowed us classifying this contact as a chalcogen intermolecular interaction being the σ*(S–C) the so-called "σ-hole" [22]. On the other side, the intermolecular contact between nitrogen and chlorine atoms is responsible for the formation of zigzag head-to-tail CCl_2FSCN chains. Adjacent chains are alternately joined through two equivalent N···S chalcogen-bond type interactions. The slight

Table 2
Relative total ΔE and free Gibbs ΔG energies (kcal mol^{-1}) and abundancies χ (%) of *anti*-conformer of CCl_2FSCN.

	ΔE^a	ΔG^a	χ^a
B3LYP/cc-pVTZ	1.15	1.12	7.3
MP2(full)/cc-pVTZ	1.13	1.11	7.4

[a] Energies are relative to those of *gauche* conformers. Gibbs free energies were calculated using standard "uncoupled harmonic rotator – rigid oscillator" approximation. The abundance was calculated from a free Gibbs energy at 305 K.

Table 3
Experimental and theoretical structural parameters of CCl_2FSCN.[a]

	gauche				*anti*		
	GED		XRD	CCSD(T)	GED		CCSD(T)
	r_e[e]	r_g[f]	r_α[g]	r_e	r_e	r_g	r_e
C1–S2	1.815(13)[1]	1.828(13)	1.822(5)	1.833	1.825(13)[1]	1.839(13)	1.844
S2–C3	1.684(8)[2]	1.690(8)	1.698(6)	1.700	1.678(8)[2]	1.685(8)	1.695
C3–N4	1.160(5)[3]	1.165(5)	1.144(9)	1.164	1.161(5)[3]	1.165(5)	1.164
C1–F5	1.338(5)[4]	1.345(5)	1.341(6)	1.338	1.345(5)[4]	1.352(5)	1.345
C1–Cl6	1.754(4)[5]	1.761(4)	1.750(4)	1.762	1.754(4)[5]	1.762(4)	1.762
C1–Cl7	1.761(4)[5]	1.770(4)	1.754(4)	1.769	1.754(4)[5]	1.762(4)	1.762
C1–S2–C3	96.5(13)[6]		97.5(2)	97.6	97.0(13)[6]		98.1
S2–C3–N4	177.1[b]		177.8(5)	177.1	177.1[b]		177.1
S2–C1–F5	110.6(3)[7]		110.9(3)	110.4	103.3(3)[7]		103.2
S2–C1–Cl6	112.0(10)[8]		113.1(3)	112.9	111.4(10)[8]		112.3
S2–C1–Cl7	107.2(24)[9]		104.9(3)	104.6	111.4(10)[8]		112.3
F5–C1–Cl6	108.5(3)[7]		107.8(4)	108.4	109.3(3)[7]		109.1
F5–C1–Cl7	109.4(3)[7]		109.2(4)	109.3	109.3(3)[7]		109.1
Cl6–C1–Cl7	109.0(28)[c]		111.0(2)	111.2	111.7(20)[c]		110.5
F5–C1–S2–C3	57.3(41)[10]		61.5(4)	62.0	180.0[b]		180.0
x,[d] %	79(11)		100	93	21(11)		7

[a] The parameters are given in Å and deg. Threefold standard deviations are in parentheses. Superscript numbers 1, 2, …, 9 indicate groups, in which parameters were refined with fixed differences. The CCSD(T) calculation was performed with cc-pVTZ basis set.
[b] Fixed parameter, see text for details.
[c] Dependent parameter.
[d] Conformational composition. Theoretical values were calculated at 305 K using the Boltzmann distribution and total energies.
[e] r_e equilibrium distance between the positions of atomic nuclei corresponding to the minimum of the potential energy.
[f] r_g average internuclear distance at the temperature of the experiment.
[g] r_α distance between vibrationally averaged positions of atoms, or better: centers of electron densities.

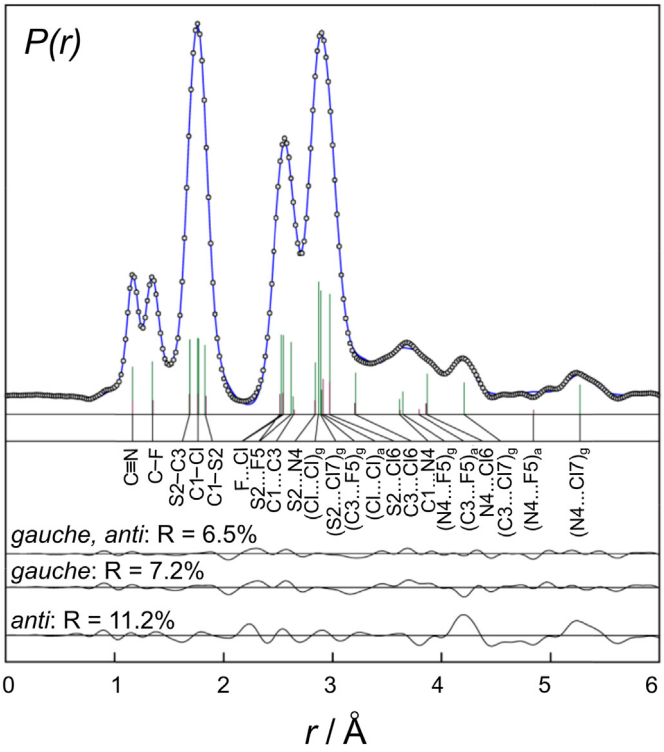

Fig. 3. Experimental (circles) and model (line) radial distribution functions of CCl_2FSCN. The difference curves for the tested models are also given. Subscript letters a and g indicate terms related only to *anti* and *gauche* conformers, correspondingly.

shortening of this bond with respect to the sum of the van der Waals radii of the involved atoms does not enable us to classify this interaction. Nevertheless, its value of 167.5° for the N···Cl–C angle and the results from the NBO calculations computing an electron donor–acceptor interaction between the nitrogen lone pair and the σ*(Cl–C) orbital, respectively, suggest that this interaction is perhaps a weak halogen contact.

Table 4
Comparison of geometrical parameters of different X–SCN compounds in the gas phase.[a]

	C≡N	C1–S2	S2–C3	C–Cl	C–S–C
gauche-CH_2Cl–SCN	1.163(3)	1.818(2)	1.698(4)	1.777(2)	99.8(15)
anti-CH_2Cl–SCN	1.164(3)	1.835(2)	1.698(4)	1.773(2)	96.5(35)
CCl_3–SCN	1.163(9)	1.839(2)	1.697(13)	1.768(2)[b]	99.9(17)
gauche-CCl_2F–SCN	1.165(5)	1.828(13)	1.690(8)	1.766(4)[b]	96.5(13)
anti-CCl_2F–SCN	1.165(5)	1.839(13)	1.685(8)	1.762(4)	97.0(13)

[a] r_g and $<_e$ geometrical parameters in Å and deg are given, if not otherwise stated, this parameters are defined in Table 3. Error estimates are three times standard deviations in this work. For definition of errors taken from literature see corresponding references.
[b] Average value.

As a consequence of the chalcogen intermolecular interaction previously described, the XRD refinement shows a "T" shaped coordination at the sulfur atom for this compound (Fig. 6). A similar coordination environment for the sulfur atom was reported for $CH_2(SCN)_2$ [23].

Chalcogen N···S interactions are also present in dichloromethyl and trichloromethylthiocyanate molecules [2,3]. N···Cl contacts are interesting to be compared as well. Evidence for this interaction is found in both, CCl_2FSCN and CCl_3SCN, but not in CH_2ClSCN.

Even though crystalline CCl_2FSCN does not show Cl···S interactions, these intermolecular contacts were detected in the other two thiocyanate species. In CH_2ClSCN this interaction presents a chalcogen-bond-type behavior, while CCl_3SCN evidences a Cl···S halogen contact.

4. Conclusion

The crystal structure of CCl_2FSCN contains solely the *gauche*-conformer while in the gas phase both *gauche*- and *anti*-conformations are present in equilibrium at room temperature, with the

Table 5
CF_2ClSCN non-bonding intermolecular interactions characteristics.

Intermolecular contact	Distance (Å)	Angle (degrees)	Sum of van der Waals radii (Å)	Shortening (Å)	Contact type proposed
N[a]···S–C(1)[b]	3.19	159.0	3.35	0.16	Chalcogen-bond
N[a]···Cl–C(1)[c]	3.25	167.5	3.30	0.05	–

[a] *x*, *y*, *z*.
[b] 1/2 + *x*, 1/2–*y*, 1–*z*.
[c] 3/2–*x*, 1–*y*, 1/2 + *z*.

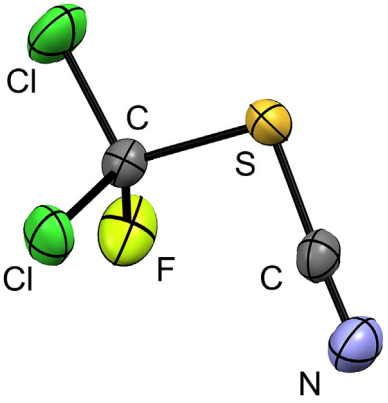

Fig. 4. Molecular structure of CCl_2FSCN in the crystal determined by X-ray diffraction at 193 K.

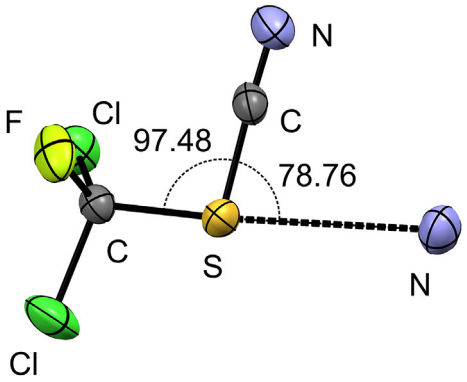

Fig. 6. T-shaped coordination environment of the sulfur atom in CCl_2FSCN.

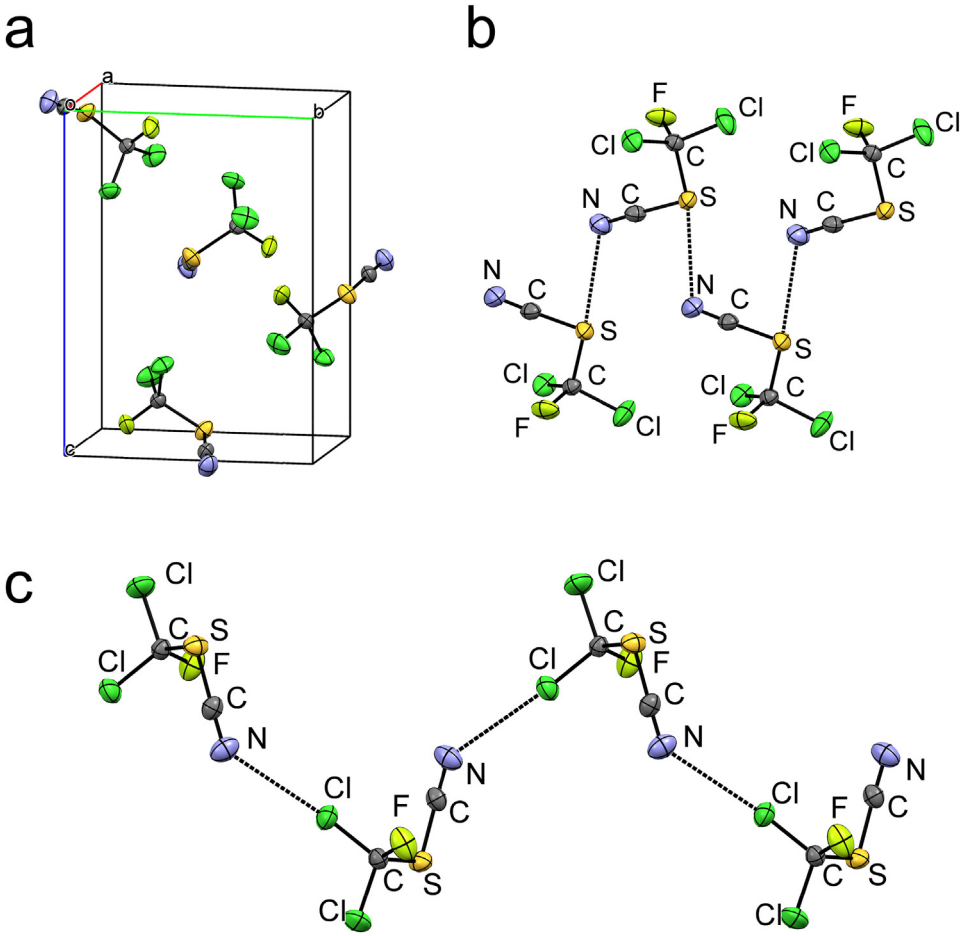

Fig. 5. a) Crystal packing and b) chalcogen and c) halogen intermolecular interactions of CCl_2FSCN determined by X-ray diffraction at 193 K.

gauche-conformer being the most stable. The parameters of the *gauche*-structure in both, solid and gas phase, are in good agreement. The C≡N bond lengths remain almost constant in CH_2ClSCN, CCl_3SCN and CCl_2FSCN in the gas phase (r_e = 1.160(5), 1.158(9), 1.160(5) Å), but they differ markedly from the solid-state values (1.145(5), 1.144(6), 1.144(9) Å, all 3 e.s.d.s), which themselves as a group are similar. This seeming systematic solid/gas difference finds its explanation in the large anisotropy of valence electron density of the terminal triply-bonded nitrogen atoms and the consequent inability of the electron-density based X-ray diffraction method to represent the nuclear position of nitrogen. The lengths of both C–S bonds are also similar in the gas and crystalline phases. The C–Cl bond lengths are also very similar within error limits in both gas and solid state, and the same applies for the C–F bond lengths. Similarly, the angles found in gas and in solid states resembles. The qualitative relationships between different parameters are the same both in crystal and in gas, despite the fact that data were acquired with a different technique in each phase and the parameters are specifically defined for each case. In the crystal structure several intermolecular interactions, in particular halogen- and chalcogen-type interactions, were observed and analyzed by means of the respective structural parameters and by quantum-chemical calculations.

Acknowledgment

The authors thank Deutsche Forschungsgemeinschaft (DFG) for the scholarship of Y. B. M. in Germany and support of the core facility GED@BI (MI 477/21-1), the Alexander von Humboldt-Stiftung (stipend for Y. V. V.), Agencia Nacional de Promoción Científica y Técnica (ANPCYT), Consejo Nacional de Investigaciones Científicas y Técnicas (CONICET), Comisión de Investigaciones de la Provincia de Buenos Aires (CIC), Facultad de Ciencias Exactas, Universidad Nacional de La Plata (UNLP) and Bielefeld University for financial support.

Appendix A. Supplementary data

Supplementary data related to this article can be found at http://dx.doi.org/10.1016/j.molstruc.2016.03.097.

Supporting information available

It contains the molecular electron scattering intensity curves (see Figs. S1–S2), the dependence of the least-squares functional value on the amount of *gauche* conformation of CCl_2FSCN (Fig. S3), experimental interatomic distances, mean square amplitudes and vibrational corrections (Tables S1–S2), the dependence of the least-squares functional value on the amount of *gauche*-conformation (Table S3) and experimental Cartesian coordinates of *gauche*- and *anti*-conformers in the gas-phase (Tables S4–S5).

References

[1] E.M. Coyanis, R.E. Rubio, K.I. Gobbato, H.-G. Mack, C.O. Della Védova, J. Mol. Struct. 344 (1995) 45–51.
[2] Berrueta Martínez, Y.; Rodríguez Pirani, L. S.; Erben, M. F.; Reuter, C. G.; Vishnevskiy, Y. V.; Stammler, H. G.; Mitzel, N. W.; Della Védova, C. O.; In preparation.
[3] Y. Berrueta Martínez, L.S. Rodríguez Pirani, M.F. Erben, C.G. Reuter, Y.V. Vishnevskiy, H.G. Stammler, N.W. Mitzel, C.O. Della Védova, Phys. Chem. Chem. Phys. 17 (2015) 15805–15812.
[4] N.N. Yarovenko, S.P. Motornyi, L.I. Kirenskaya, Zh. Obshch. Khim 29 (1959) 3789.
[5] H. Brintzinger, K. Pfannstiel, H. Koddebusch, K.E. Kling, Chem. Ber. 83 (1950) 87–90.
[6] M.J. Frisch, G.W. Trucks, H.B. Schlegel, G.E. Scuseria, M.A. Robb, J.R. Cheeseman, J.A. Montgomery Jr., T. Vreven, K.N. Kudin, J.C. Burant, J.M. Millam, S.S. Iyengar, J. Tomasi, V. Barone, B. Mennucci, M. Cossi, G. Scalmani, N. Rega, G.A. Petersson, H. Nakatsuji, M. Hada, M. Ehara, K. Toyota, R. Fukuda, J. Hasegawa, M. Ishida, T. Nakajima, Y. Honda, O. Kitao, H. Nakai, M. Klene, X. Li, J.E. Knox, H.P. Hratchian, J.B. Cross, V. Bakken, C. Adamo, J. Jaramillo, R. Gomperts, R.E. Stratmann, O. Yazyev, A.J. Austin, R. Cammi, C. Pomelli, J.W. Ochterski, P.Y. Ayala, K. Morokuma, G.A. Voth, P. Salvador, J.J. Dannenberg, V.G. Zakrzewski, S. Dapprich, A.D. Daniels, M.C. Strain, O. Farkas, D.K. Malick, A.D. Rabuck, K. Raghavachari, J.B. Foresman, J.V. Ortiz, Q. Cui, A.G. Baboul, S. Clifford, J. Cioslowski, B.B. Stefanov, G. Liu, A. Liashenko, P. Piskorz, I. Komaromi, R.L. Martin, D.J. Fox, T. Keith, M.A. Al-Laham, C.Y. Peng, A. Nanayakkara, M. Challacombe, P.M.W. Gill, B. Johnson, W. Chen, M.W. Wong, C. Gonzalez, J.A. Pople, Gaussian 03, Revision C.02, Gaussian, Inc., Wallingford CT, 2004.
[7] Parr, R. G.; Yang, W.; Oxford University Press, New York, USA, 1989.
[8] C. Møller, M.S. Plesset, Phys. Rev. 46 (1934) 618–622.
[9] V.A. Sipachev, J. Mol. Struct. 693 (2004) 235–240.
[10] Sipachev, V. A.; 2001, 567–568, 67–72.
[11] V.A. Sipachev, Struct. Chem. 11 (2000) 167–172.
[12] K. Raghavachari, G.W. Trucks, J.A. Pople, M. Head-Gordon, Chem. Phys. Lett. 157 (1989) 479–483.
[13] M.E. Harding, T. Metzroth, J. Gauss, A.A. Auer, J. Chem. Theory Comput. 4 (2008) 64–74.
[14] J.P. Foster, F. Weinhold, J. Am. Chem. Soc. 102 (1980) 7211–7218.
[15] a) R.J.F. Berger, M. Hoffmann, S.A. Hayes, N.W. Mitzel, Z. Naturforsch 64b (2009) 1259–1268;
b) C.G. Reuter, Yu V. Vishnevskiy, S. Blomeyer, N.W. Mitzel, Z. Naturforsch 71b (2016) 1–13.
[16] Yu V. Vishnevskiy, J. Mol. Struct. 833 (2007) 30–41.
[17] Yu V. Vishnevskiy, J. Mol. Struct. 871 (2007) 24–32.
[18] R. Boese, M. Nussbaumer, in: D.W. Jones, A. Katrusiak (Eds.), Correlations, Transformations, and Interactions in Organic Crystal Chemistry, 7, IUCr Crystallographic Symposia, Oxford, 1994, pp. 20–37.
[19] G.M. Sheldrick, Acta Crystallogr. A 64 (2008) 112–122.
[20] D. Brodalla, D. Mootz, R. Boese, W. Osswald, J. Appl. Crystallogr. 18 (1985) 316–319.
[21] B.J. Lynch, D.G. Truhlar, J. Phys. Chem. A 105 (2001) 2936–2941.
[22] [a] R.G. Gonnade, M.S. Shashidhar, M.M.J. Bhadbhadev, Ind. Inst. Sci. 87 (2007) 149–165;
[b] P. Politzer, J.S. Murray, Chem. Phys. Chem. 14 (2013) 278–294;
[c] J.S. Murray, P. Politzer, T. Clark, Phys. Chem. Chem. Phys. 15 (2013) 11178–11189.
[23] J.H. Konnert, D. Britton, Acta Crystallogr. Sect. B 27 (1971) 781–786.